Observation of THz evanescent waves in a Smith-Purcell free-electron laser

H. L. Andrews,* C. A. Brau, and J. D. Jarvis
Department of Physics and Astronomy, Vanderbilt University, Nashville, Tennessee 37235, USA

C. F. Guertin, A. O'Donnell, B. Durant, T. H. Lowell, and M. R. Mross
Vermont Photonics, Bellows Falls, Vermont 05101, USA
(Received 4 March 2009; published 19 August 2009)

We present experimental observations of evanescent waves in a Smith-Purcell free-electron laser (FEL). These waves, predicted by both theory and simulations, have wavelengths longer than the Smith-Purcell radiation, group velocity antiparallel to the electron beam, and for sufficiently high current, provide feedback to bunch the electron beam. This feedback is the basis of oscillator operation of the Smith-Purcell FEL. The wavelengths observed agree with theoretical predictions, and strong radiation from the upstream end of the grating confirms the negative group velocity. Radiation observed at the second harmonic may indicate electron bunching by the evanescent wave.

DOI: 10.1103/PhysRevSTAB.12.080703 PACS numbers: 41.60.Cr, 07.57.Hm, 84.40.Fe

I. INTRODUCTION

Given the historic paucity of compact, narrowband, tunable sources in the far-infrared, or terahertz (THz), region, there has been a long-standing interest in developing such a source for applications in fields such as biology, chemistry, and materials science [1,2]. Devices consisting of a metal grating and electron beam have widely been proposed as candidates for such a source. When an electron beam travels over a conducting periodic structure, it excites both an evanescent wave and spontaneous Smith-Purcell radiation [3]. The former is characteristic of all slow wave structures. The later is distinguished by the dependence of the wavelength λ on the grating period L, normalized electron velocity $\beta = v/c$ where v is velocity and c is the speed of light, order number of the radiation n and angle of observation θ measured from the electron beam,

$$\lambda = \frac{L}{|n|}\left(\frac{1}{\beta} - \cos\theta\right). \quad (1)$$

Many varieties of grating based compact free-electron lasers have utilized one or both of these emissions. Such devices include backward-wave oscillators (BWO) [4,5], traveling-wave tubes [4], ledatrons [6], orotrons [7], and planar orotrons [8]. The differences between these devices either lie with the structure surrounding the grating, or whether the device primarily uses the evanescent mode or the Smith-Purcell radiation for feedback. The device investigated here, called a Smith-Purcell free-electron laser (SPFEL), consists of a grating, with or without conducting vertical sidewalls, and an electron beam. It uses oscillation of the evanescent wave, which occurs above the start current, to bunch the electron beam and excite harmonics of the evanescent frequency which fall in the Smith-Purcell band and therefore radiate.

Over the past decade the two-dimensional theory of operation of the SPFEL has developed to a point where theories from separate institutions agree well with each other, with simulations performed with particle-in-cell (PIC) codes such as MAGIC [9–15], and with experiments using a sheet electron beam [16,17]. The three-dimensional theories with and without grating sidewalls have also been shown to agree well with PIC code simulations [18–20]. Prior experiments using a cylindrical electron beam have not observed the evanescent wave [21,22]; however, neither collected emission in a way that would allow them to detect it, and neither operated above the predicted start current. This work presents the first experimental observations of evanescent waves at THz frequencies in an SPFEL with grating sidewalls, the first key step toward demonstrating lasing of an SPFEL.

II. THEORETICAL PREDICTIONS

The wavelength of the evanescent wave is longer than that of the lowest Smith-Purcell band, so the wave is emitted by scattering at the ends of the grating. The evanescent wave has a phase velocity matching the electron beam velocity, but its group velocity can be either parallel or antiparallel to the electron beam depending on the grating parameters and beam energy. For the case of negative group velocity, SPFEL operation is very much like a BWO. The wave grows as it travels upstream, so each electron entering the grating encounters a more intense field and interacts more strongly. In this manner, the evanescent wave bunches the electrons and provides its own feedback. For sufficiently high electron-beam current, the growth rate of the field overcomes Ohmic losses and the field grows exponentially. The 2D theory includes these

*Corresponding author.
heather.l.andrews@vanderbilt.edu

losses and shows that losses increase and eventually overtake gain for all current levels as the group velocity decreases to zero at the Bragg point [12]. Though the 3D theory with sidewalls does not include losses, we expect the same behavior near the Bragg point. For the 3D case, the presence of sidewalls both confines the evanescent modes to increase interaction with a round profile electron beam and increases the collection efficiency of the spontaneous radiation. In a BWO, the evanescent wave is collected as the output, but for an SPFEL, the evanescent wave bunches the electron beam strongly enough to excite higher harmonics whose wavelengths fall in the radiative Smith-Purcell bands. This way various wavelengths can be produced in the same device. The evanescent wave is collected when it scatters at the grating ends, and the shorter wavelength harmonics can be collected more efficiently as they radiate. A complete description of this theory can be found in [18,23].

A grating with sidewalls supports an infinite set of transverse evanescent modes, denoted by $r = 0, 1, 2 \ldots$. A plot of the dispersion diagram for grating VBLT-001 (period 157 μm, slot width 48 μm, slot depth 228 μm, length 50 periods, width 500 μm) is shown in Fig. 1. Dispersion relations predicted by the 2D theory [10] and the first four transverse modes from the 3D theory with sidewalls [18] are shown. The intersection point of the dispersion curve and beam line determines the wavelength of the evanescent wave. The group velocity of the wave is given by the slope of the dispersion curve at the intersection. For this grating the 2D theory predicts a wavelength around 900 μm and positive group velocity. The 3D theory predicts a wavelength of about 790 μm for the lowest ($r = 0$) mode and about 640 μm for the next highest ($r = 1$) mode. Both predicted 3D modes indicate a negative group velocity, a remarkable difference from the 2D theory. The start current predicted at 34 kV is 5 mA for the $r = 0$ mode and 350 mA for the $r = 1$ mode when Ohmic losses are ignored. Even though the start current for oscillation of the $r = 1$ mode is very high, we expect the mode to be present.

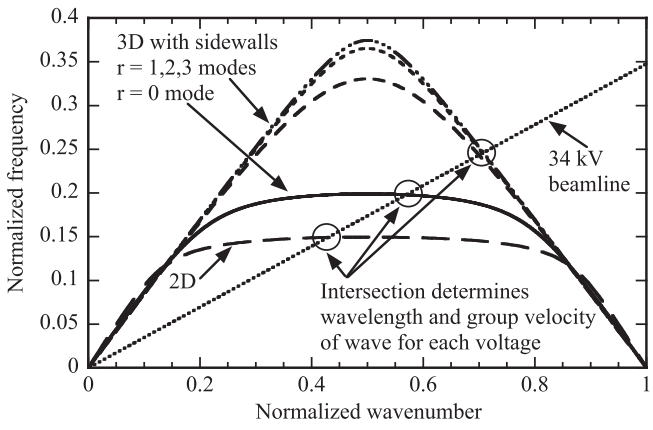

FIG. 1. Theoretical predictions for the dispersion relations for grating VBLT-001 by the 2D theory and 3D theory with walls. The intersection of the beam line and dispersion relation predict the wavelength and group velocity of the evanescent wave. The 2D theory predicts a longer wavelength and opposite group velocity compared to the 3D theory. Wavelength and wave number were normalized by $L/2\pi$.

III. EXPERIMENT DETAILS

Experiments were conducted at Vermont Photonics. As shown in Fig. 2 the apparatus used is based on a scanning electron microscope design [24]. The electron beam originates at a lanthanum hexaboride (LaB_6) thermionic cathode. The emission current level is controlled by a cathode heater and a wehnelt (or extractor) potential. The beam is accelerated by an anode, and passes through two focusing lenses used to adjust the position and depth of focus. The position of the beam over the grating is controlled by steering coils (not shown). In typical experiments, a voltage and current are selected, then the steering coils and lenses are adjusted to position the beam over the grating to maximize output radiation. The electron-beam voltage range for these experiments was 26–38 kV. The apparatus can produce beam currents between 0.3–17 mA, but measurements presented here were taken at 5–10 mA, near the

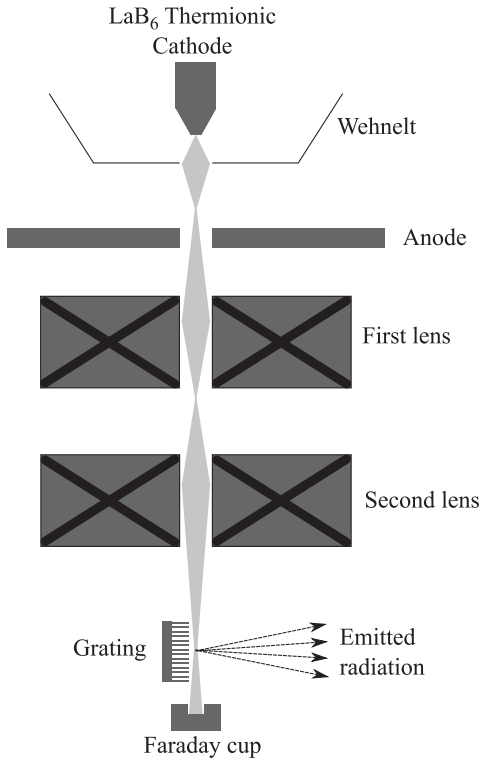

FIG. 2. The electron beam originates at a LaB_6 thermionic cathode. The current is controlled by heater current and wehnelt bias voltage. Beam energies range 26–38 kV, beam currents 0.3–17 mA. The beam is focused by magnetic lenses and directed perpendicular to the direction of travel by steering coils (not shown).

predicted start current for this design. To minimize grating heating, the beam is pulsed at 10 Hz with a 10% duty factor. From simulations and aperture measurements we determined the beam radius is approximately 25 μm. From these measurements, we estimate the beam emittance to be 0.4 mm mrad. Though we are unable to measure the height of the beam above the grating, we infer, from damage observed in the grating after runs, that for most cases the beam skims the grating surface. While there is a slow drift in the vertical beam position, which changes the overall output power level, it takes place on a time scale long compared with that for collecting a few spectra. By monitoring the overall power level any changes caused by this drift can be minimized.

The path of radiation emitted from the grating is shown in Fig. 3. Emission is collected and collimated by a one-inch diameter off-axis paraboloid mirror, with a collection angle of $\pm 20°$, and directed through the output window of the vacuum chamber. The mirror position, with respect to the grating, can be adjusted by an external motor. In this way the mirror can be set to collimate emission from either the upstream, middle, or downstream part of the grating, with respect to the electron beam. This flexibility allows us to observe both radiation emitted into some range of angles off the grating, or scattered from the ends of the grating. The collimated output radiation is directed into a Michelson Fourier-transform infrared (FTIR) interferometer, and then into a composite silicon bolometer fitted with a 200 μm long-pass filter. Interferograms were transformed using the Mertz method fast Fourier-transform technique [25]. In this process they were also normalized by dividing the maximum detector signal through the FTIR by the area under the spectrum, so that spectra taken under different conditions can be compared reliably. The two to three spectra typically taken under identical conditions were averaged to yield the data presented here.

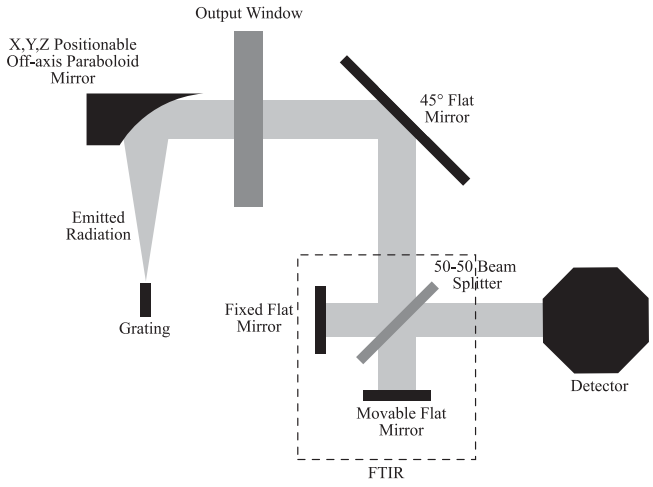

FIG. 3. Radiation produced by the grating is collected and collimated by an off-axis paraboloidal mirror, directed out of the vacuum chamber, through a Michelson FTIR interferometer and into a composite silicon bolometer. In this diagram the electron beam runs into the page above the grating.

All gratings used are fabricated out of copper, have a rectangular profile, and are equipped with smooth vertical sidewalls extending at least 500 μm above the grating surface [26]. Two distinct grating geometries were used. The first, denoted W-048 (period 157 μm, slot width 25 μm, slot depth 122 μm, length 40 periods, width 610 μm), was a design frequently used at Vermont Photonics before this collaboration. The grating denoted VBLT-001 (period 157 μm, slot width 48 μm, slot depth 228 μm, length 50 periods, width 500 μm) was designed to maximize the evanescent wave output predicted by the 3D theory with grating sidewalls. Four instances of VBLT-001 were used. Because of the manufacturing process, the actual grating parameters were not uniform over one grating, and varied over all the gratings by up to 10 μm from the parameters given.

IV. RESULTS AND DISCUSSION

The evanescent wave was observed with both the W-048 and VBLT-001 gratings, but only data taken with VBLT-001 are shown. Though the full 180° predicted Smith-Purcell band at 34 kV for both gratings is 295–605 μm, only a fraction of this spectrum is observed. The observed Smith-Purcell range agrees well with the $\pm 20°$ acceptance angle of the collection optics. For VBLT-001 we operated near the predicted start current of the $r = 0$ mode for all experiments. For W-048 we operated far below the predicted start current of 450 mA, but unlike prior experiments [21,22] we observed the ends of the grating for scattered emission. The evanescent waves are present far below the start current, but they do not have gain sufficient to bunch the beam. Similar to the experiments mentioned above, there was substantial heating of the grating, but this did not effect the results. We observed narrow spectral features, clearly distinct from noise, while the broad spectral signature of blackbody emission was absent.

One of the most unexpected observations was that of the $r = 1$ mode, shown along with the $r = 0$ mode and spontaneous Smith-Purcell radiation in Fig. 4. Until this experiment it was assumed that the group velocity of this mode was too high for it to have any significant interaction with the electron beam. It is possible that this mode appears dominant in some cases because the group velocity is large enough to transport substantial power to the upstream end of the grating where it scatters and can be detected.

We also observed much stronger emission when the mirror was positioned to collect radiation from the upstream end of the grating than when it was positioned to collect from the downstream end as shown in Fig. 5. For this plot only the $r = 0$ is present, and the emission is much stronger with the mirror in the upstream position. A similar disparity in emission was also observed for the $r = 1$ mode. This disparity of radiation intensity indicates that

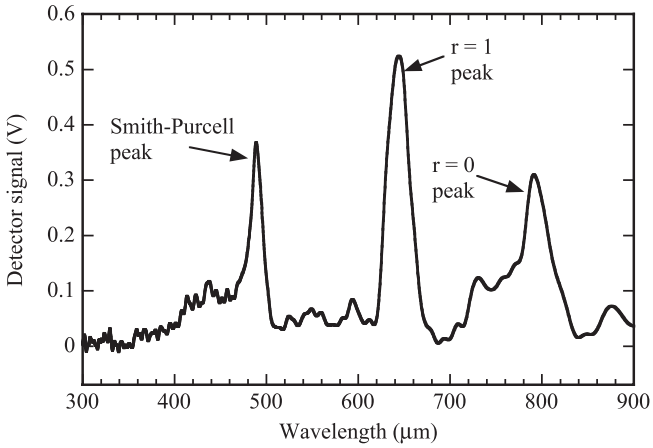

FIG. 4. Spectrum taken at 34 kV showing the Smith-Purcell band from 420–500 μm, the $r = 1$ mode at 645 μm, and the $r = 0$ mode at 790 μm. These data were collected from the upstream end of the grating.

the evanescent modes are backward waves, in agreement with the 3D theory including walls.

The wavelength and intensity of the evanescent modes was observed to change with increasing voltage as predicted. Figure 6 shows the $r = 1$ mode at 30, 34, and 38 kV at the upstream end of the grating and Fig. 7 shows the $r = 0$ mode at 30 and 34 kV at the downstream end of the grating. For the $r = 1$ mode, wavelengths become shorter with increasing voltage, and for the $r = 0$ mode, there is a slight wavelength shift and strong emission increase. Both behaviors are explained by considering the dispersion diagram of the 3D theory in Fig. 1. For the $r = 0$ mode, as the beam voltage increases the slope of the beam line increases and the intersection point moves to slightly shorter wavelength and lower group velocity. The gain will increase with decreasing group velocity, until Ohmic losses dominate for very low group velocity, as mentioned earlier. For

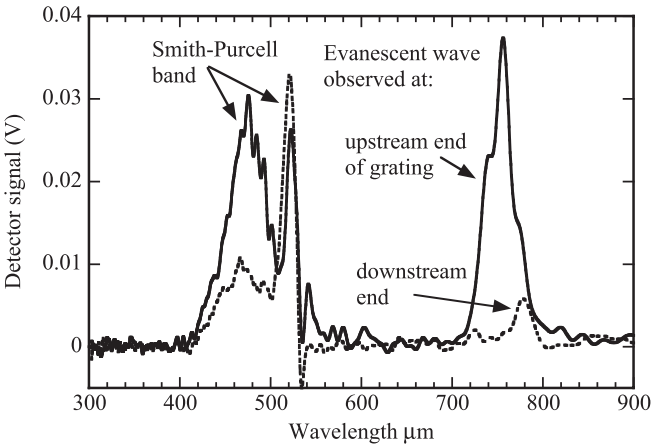

FIG. 5. Spectra taken at 30 kV with the mirror centered on the upstream (solid) and downstream (dotted) end of the grating. As predicted by the 3D theory, the evanescent wave is much stronger at the upstream end, indicating a backward wave.

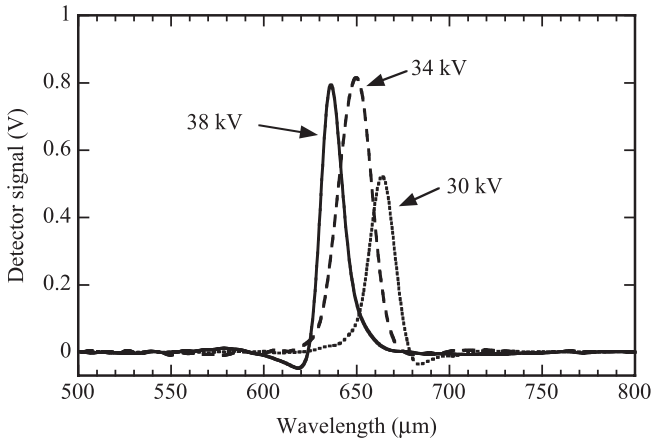

FIG. 6. The $r = 1$ mode shifts to shorter wavelength with increasing voltage as predicted. Spectra were collected at the upstream end of the grating.

the $r = 1$ mode, the group velocity is nearly constant, so no change in intensity is expected, but the intersection point shifts to measurably shorter wavelength. In Fig. 7 there is also a peak around 375 μm that may correspond to the second harmonic of the $r = 0$ mode. This peak is outside the range of the collection optics and should only be observed when the evanescent wave is particularly strong. Its presence suggests that there may be sufficient beam bunching by the $r = 0$ mode to excite the second harmonic to detectable levels.

The agreement between predicted and observed wavelengths is very good. This can be seen in Fig. 8 where solid lines denote predicted wavelengths for the $r = 0$ and $r = 1$ modes. Solid diamonds and triangles, respectively, denote observed values for the $r = 0$ and $r = 1$ modes. Dotted lines above and below the predicted wavelengths indicate a

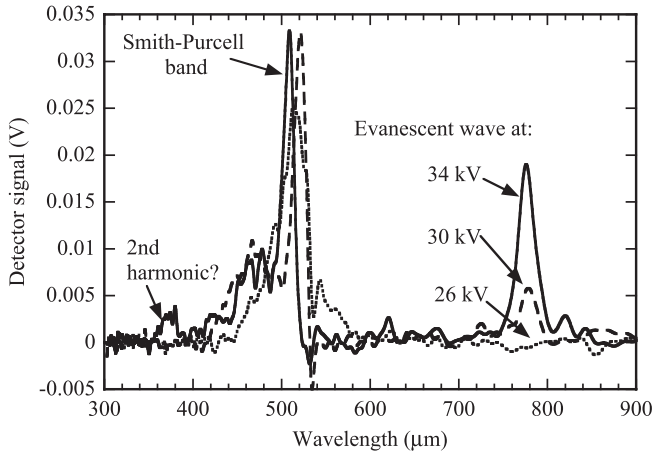

FIG. 7. The $r = 0$ mode increases in intensity and shows a slight shift to shorter wavelength with increasing voltage as expected. In the 34 kV spectrum there is another peak near 375 μm, the second harmonic of the $r = 0$ mode. Its presence may suggest beam bunching. Spectra were collected at the downstream end of the grating.

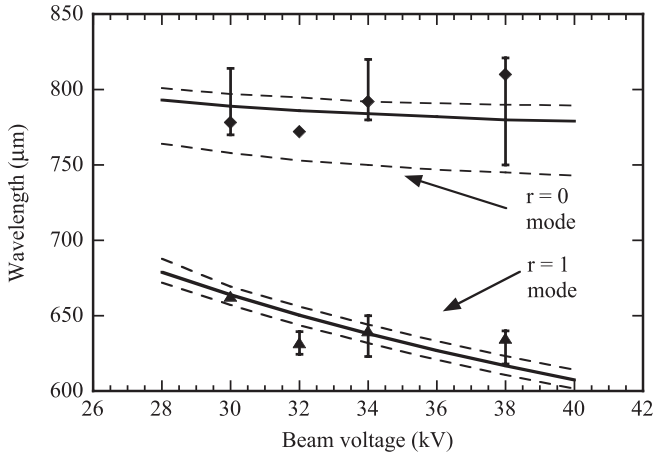

FIG. 8. Predicted (solid lines) and observed wavelengths over a range of voltages for $r = 0$ (diamonds) and $r = 1$ (triangles) modes. Dashed lines indicate variability in predictions due to variation in actual grating dimensions, while error bars on the data points represent the spread of observed wavelengths.

variance in predicted values due to variation in the actual grating parameters, and error bars on the data points indicate the range of observed wavelengths.

While there was quite a variance in total power and spectral composition from one run to the next, even for seemingly identical control parameters, the data presented here illustrate the reproducible features of the observed emission. Some of the differences can be attributed to differences in grating parameters, system alignment, and beam profile, but there is much left to do to understand the causes of these variations.

V. CONCLUSIONS AND FURTHER WORK

We present experimental observations of evanescent waves in a SPFEL. These waves are predicted by both analytic theories and particle-in-cell code simulations. The wavelengths observed agree well with those predicted by the most recent three-dimensional theory for a grating with flat, vertical sidewalls. We may also have observed indications of beam bunching by the evanescent wave. To induce lasing in the SPFEL, we plan to use more finely machined gratings and redesign the output optics to collect emission at both the fundamental and second harmonic more efficiently.

ACKNOWLEDGMENTS

The authors gratefully acknowledge helpful discussions with Dazhi Li and Jack Donohue.

[1] P. H. Siegel, IEEE Trans. Microwave Theory Tech. **50**, 910 (2002).
[2] S. P. Mickan and X.-C. Zhang, Int. J. High Speed Electron. Syst. **13**, 601 (2003).
[3] S. J. Smith and E. M. Purcell, Phys. Rev. **92**, 1069 (1953).
[4] J. Pierce, *Travelling-Wave Tubes* (D. Van Nostrand Company, Inc., New York, 1950).
[5] H. R. Johnson, Proc. IRE **43**, 684 (1955).
[6] K. Mizuno, S. Ono, and Y. Shibata, IEEE Trans. Electron Devices **20**, 749 (1973).
[7] F. S. Rusin and G. D. Bogomolov, Proc. IEEE **57**, 720 (1969).
[8] E. M. Marshall, P. M. Phillips, and J. E. Walsh, IEEE Trans. Plasma Sci. **16**, 199 (1988).
[9] C. S. Liu and V. K. Tripathi, IEEE J. Quantum Electron. **35**, 1386 (1999).
[10] H. L. Andrews and C. A. Brau, Phys. Rev. ST Accel. Beams **7**, 070701 (2004).
[11] V. Kumar and K.-J. Kim, Phys. Rev. E **73**, 026501 (2006).
[12] H. L. Andrews, C. H. Boulware, C. A. Brau, J. T. Donohue, J. Gardelle, and J. D. Jarvis, New J. Phys. **8**, 289 (2006).
[13] J. T. Donohue and J. Gardelle, Phys. Rev. ST Accel. Beams **8**, 060702 (2005).
[14] D. Li, Z. Yang, K. Imasaki, and G.-S. Park, Phys. Rev. ST Accel. Beams **9**, 040701 (2006).
[15] J. Gardelle and J. T. Donohue, IEEE Trans. Electron Devices **56**, 769 (2009).
[16] B. K. Skrynnik, V. K. Korneyenkov, and M. Y. Demchenko, Telecommun. Radio Eng. **55**, 170 (2001).
[17] J. Gardelle, L. Courtois, P. Modin, and J. T. Donohue (unpublished).
[18] H. L. Andrews, J. D. Jarvis, and C. A. Brau, J. Appl. Phys. **105**, 024904 (2009).
[19] D. Li, K. Imasaki, X. Gao, Z. Yang, and G.-S. Park, Appl. Phys. Lett. **91**, 221506 (2007).
[20] D. Li, K. Imasaki, Z. Yang, and G.-S. Park, Appl. Phys. Lett. **88**, 201501 (2006).
[21] J. Urata, M. Goldstein, M. F. Kimmitt, A. Naumov, C. Platt, and J. E. Walsh, Phys. Rev. Lett. **80**, 516 (1998).
[22] O. H. Kapp, Y. Sun, K.-J. Kim, and A. V. Crewe, Rev. Sci. Instrum. **75**, 4732 (2004).
[23] H. L. Andrews, C. H. Boulware, C. A. Brau, and J. D. Jarvis, Phys. Rev. ST Accel. Beams **8**, 110702 (2005).
[24] M. Mross, T. H. Lowell, R. Durant, and M. F. Kimmitt, J. Biol. Phys. **29**, 295 (2003).
[25] P. R. Griffiths and J. A. de Haseth, *Fourier Transform Infrared Spectrometry* (John Wiley and Sons, Inc., New York, 1986).
[26] A. Bakhtyari and J. H. Brownell, Appl. Phys. Lett. **82**, 3150 (2003).